PAPER • **OPEN ACCESS**

Influence of annealing on optical and photovoltaic properties of nanostructured TiO_2 films

To cite this article: T M Serikov *et al* 2017 *IOP Conf. Ser.: Mater. Sci. Eng.* **168** 012054

Influence of annealing on optical and photovoltaic properties of nanostructured TiO_2 films

T M Serikov[1], N Kh Ibrayev[1], Zh Kh Smagulov[1] and K.A. Kuterbekov[2]
[1] Karaganda, 100028, Republic of Kazakhstan, Institute of Molecular Nanophotonics, E.A. Buketov Karaganda State University
[2] Astana, 010000, Republic of Kazakhstan, L.N. Gumilyov Eurasian National University

E-mail: serikov-timur@mail.ru

Abstract. Spectral and kinetic characteristics of the photoluminescence of TiO_2 films obtained from TiO_2 nanoparticles and nanotubes were studied. Luminescence spectra typical for the TiO_2 with anatase structure were observed under UV excitation of the films. Heat treatment of the films at T=1273 K leads to a long-wavelength shift of the photoluminescence band with maximum at 850 nm, which corresponds to the rutile structure. The luminescence duration of rutile films is longer than the luminescence duration of the anatase films as for nanoparticles and for nanotubes. The photovoltaic properties of TiO_2 films with different structures were investigated. It was established that anatase structured films have a higher photocurrent than the rutile structured film. By impedance spectroscopy method it was found that the electron transport resistance in the nanotube films is higher but the recombination rate is lower than in the TiO_2 nanoparticle films.

1. Introduction

Titanium dioxide (TiO_2) - belongs to a class of wide-band semiconductors widely used in photocatalysis, medicine, ecology, and dye-sensitized solar cells (DSSC) [1-4]. The speed of electrons transport through the oxide semiconductor to the collecting electrode has a great importance for efficient operation of solar cells. Using the various methods we can get TiO_2 nanostructures in the form of nanoparticles (NPs) [6], nanotubes (NTs) [7], nanorods [8] and nanowires [9]. In DSSC TiO_2 NPs are the most commonly used. However, the relationship between the NPs formed by thermal annealing, affects the ability of electron transition from nanoparticle to nanoparticle. Unformed contacts lead to a decrease in the efficiency of electron transport. When using NTs one-dimensional electrons transport is possible along the sides. In addition, with proper design of the electrodes there will be fewer defects hindering electrons transport [10]. The presence of defects in nanostructures can create additional trapped levels of energy in the forbidden gap. Defects in the TiO_2 crystal lattice have a significant impact on its optical and electrical properties that can affect the efficiency of converting solar energy into electrical one. Therefore, the need to obtain information about the defect states in the bulk and on the surface of TiO_2 nanostructures is essential [11-13]. One of the sensitive methods in the study of structural defects is photoluminescence spectroscopy. It is characterized by high sensitivity to the presence of impurities and defects in the crystalline structure that alter the spectral composition and intensity of the luminescence. There is a number of papers devoted to the study of defects in nanostructures of titanium dioxide [14-17]. It should be noted that the majority of studies were

performed for the anatase and rutile of titanium dioxide nanoparticles [18]. Luminescence centers of titanium dioxide nanotubes obtained by electrochemical anodization, remains little explored. This paper presents the results of studies of the effect of heat treatment of films formed by NTs titanium dioxide on their luminescent and electrophysical properties.

2. Experimental part

2.1. Obtaining films from NPs TiO_2

Colloidal TiO_2 powder (Sigma Aldrich) was triturated in a porcelain mortar with deionized water and acetone in a volume ratio of 10:1. After the formation of a homogeneous viscous paste NPs solution of titanium dioxide was deposited on the substrate surface by the doctor-blading method. For optical measurements polished plates from non-luminescent quartz were used. For measurements of current-voltage characteristics (CVC) glass plates with a conductive layer of the FTO (glass coated with tin oxide doped with fluorine) were used. The average size of NPs is ~ 21 nm. The resulting films were subjected to heat treatment at a temperature of 773 and 1273 K during 2 hours.

2.2. Synthesis of NTs TiO_2

The titanium foil with a thickness of 60 microns was subjected to chemical polishing. As the basis of electrolyte the $C_2H_6O_2$ was used (content of NH_4F is 0,5 wt%, H_2O is 3 wt%). Anodic oxidation of titanium was carried out in an electrochemical cell in potentiostatic mode at a temperature of 5-7 ^{0}C. The platinum foil was as a cathode. The distance between the anode and cathode was 3 cm.

The electrochemical oxidation process consists from three steps. First is anodizing for 2 hours. Separation the formed film at the first step is carried out in an ultrasonic bath of 1 M hydrochloric acid solution. Then the sample was washed with copious amounts of deionized water and dried at a temperature of 80 ^{0}C. The duration of the second step of anodizing was 24 hours. Anodizing voltage was 50 V. After the second stage of the anodizing the obtained TiO_2 nanotubes were sonicated to remove the byproducts and the surface oxide layer. Then they were washed with copious amounts of distilled water and dried in a stream of nitrogen. Crystallization of the amorphous phase of TiO_2 was performed by the thermal treatment of samples in a muffle furnace at 450 ° C for 2 hours with a temperature increase of 5 ^{0}C per minute. The third stage of the anodizing was used for films separation formed by the NTs titanium dioxide from titanium foil [20]. Anodizing was carried out at a temperature of electrolyte of 70^{0}C and the voltage of 60 V. The process came to an independent film separation from the titanium foil. Then, the resulting films were subjected to heat treatment at a temperature of 773 and 1273 K during 2 hours. The images of samples surface were obtained on the scanning electron microscope MIRA 3LMU (Tescan, Czech Republic). Measurements of spectral and kinetic characteristics of the films were carried out on an automated spectral and kinetic installation with registration in photon counting mode at the boiling point of liquid nitrogen. Excitation was carried out by a nitrogen laser AIL -3 (λ_{gen} = 337 nm, E = 30 mJ, τ_p= 10 ns). Before measurement the sample was placed in an optical cryostat, which had previously been evacuated to a residual pressure.

2.3. Assembling DSSC

Solar cells based on NPs and NTs titanium dioxide were obtained following the procedure described in the paper [21, 22]. To increase the spectral sensitivity range the ruthenium dye N719 was used (Di-tetrabutylammonium cis-bis (isothiocyanato) bis (2.2’ - bipyridyl - 4.4’ - dicarboxylato) ruthenium (II), Sigma Aldrich). Sorption occurred within 24 hours. Platinum electrodes were deposited from an ethanol solution H_2PtCl_6 by the electrochemical method on FTO. Gasket between the electrodes served the film Meltonix (Solaronix, Switzerland) with 30 microns thick. As electrolyte Iodolyte H30 (Solaronix, Switzerland) was used. IV-characteristics of solar cells were measured under illumination of cells with light of xenon lamp with a light output of 100 mW / cm^2 (Air Mass (AM) 1.5) at the measuring complex CT50AAA (PET PHOTO Emission TECH. INC., USA). Spectra of electrochemical cell impedance was measured under standard simulated solar radiation (Air Mass

(AM) 1.5) at Z-500PRO (Elins, Russia). The amplitude of the applied sinusoidal signal was 20 mV and the frequency was varied from 1 MHz to 100 MHz.

3. Results and discussion

It is known that before NTs heat treatment, TiO_2 structure is amorphous [23]. Crystallization of the structure occurs during thermal annealing of the sample, starting with the temperature of 553K. At a temperature of 773 K the amorphous phase proceeds anatase structure. At further annealing to 1273 K anatase structure is completely transformed into the rutile phase. The morphology of the films surface formed by the NPs and NTs titanium dioxide and heat-treated at a temperature of 773 and 1273 K is shown in Figure 1.

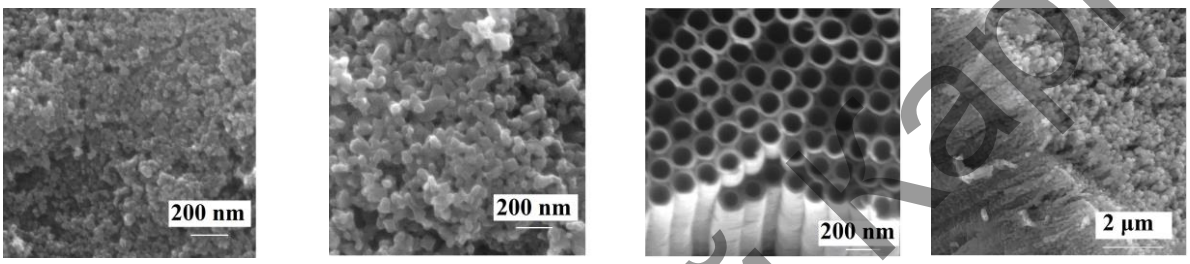

а) б) в) г)

Figure 1. SEM images of the titanium dioxide films.

From Figure 1, a and 1, b it is seen that the films from NPs titanium dioxide have distinct granular structure. For the same magnification it is noticeable that the film annealed at 1273 K consists of larger particles than the film that had been subjected to thermal annealing at a temperature of 773 K. This is probably due to the fact that under high temperature some of the particles sintered forming larger agglomerates. Figure 1 shows a SEM image of a film formed by TiO_2 NTs. The figure shows that NTs are tightly packed and their ends are open. Increase of the annealing temperature up to 1273 K also results in a significant change of the structure (Fig. 1, d). It is evident that although the film retains a tubular structure, the open channels are not observed on the surface. Figure 2 shows the luminescence spectra and kinetics of films luminescence decay of anatase structure formed by the NPs and NTs titanium dioxide.

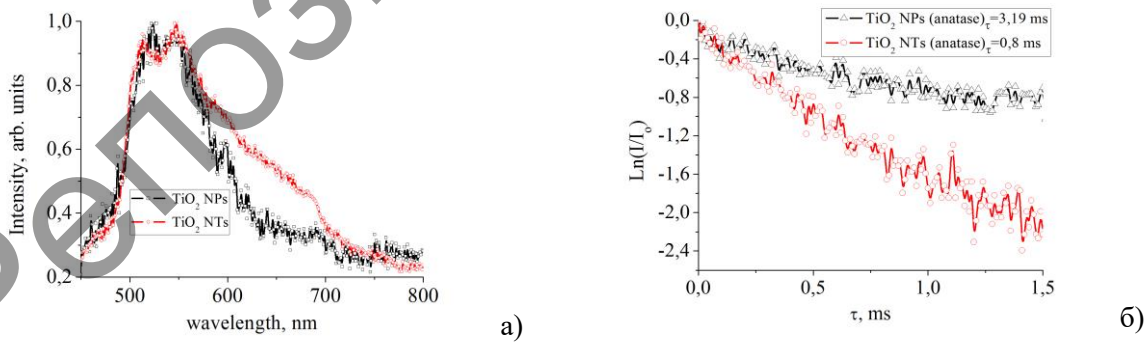

а) б)

Figure 2. Normalized luminescence spectra (a) and luminescence kinetics (b) of anatase films formed by NPs and NTs titanium dioxide.

At room temperature luminescence was not observed for both samples. When cooling film to T=160 K in the wavelength range of 400 - 800 nm a broad band of emission from maximum 510 and 540 nm is recorded. By lowering the substrate temperature to 90 K the intensity of the luminescence increases. The nature of this luminescence is associated with defects located in the surface area of the crystallites [23]. From a comparison of the luminescence spectra it is evident that in NTs luminescence intensity of 600-700 nm is higher than in the case of NPs. Using the approximation by the Gaussian

functions luminescence spectra were divided into components, the form of which is shown in Figure 3. The results of approximation show that the observed luminescence spectra are formed by three bands with maximum at 510, 540 and 600 nm.

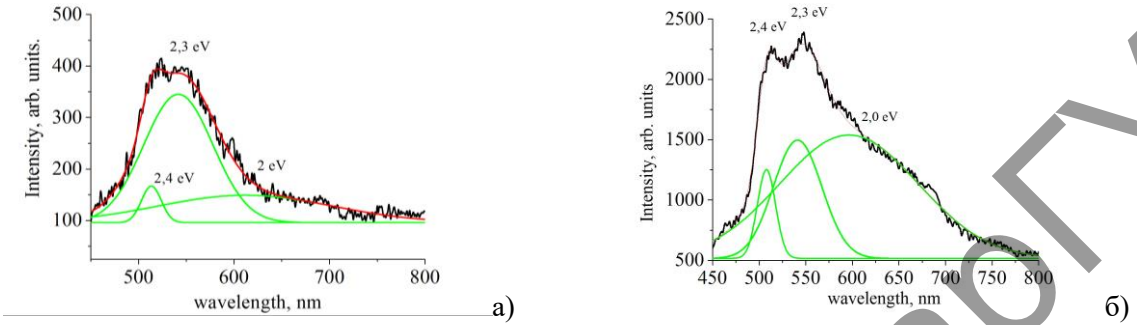

а) NPs TiO_2 (773 K); б) NTs TiO_2 (773 K)

Figure 3. Gaussian approximation of the photoluminescence spectrum of nanoparticles and nanotubes of titanium dioxide measured at 90 K.

For all of the observed defect luminescence centers the kinetics of luminescence decay were measured. Figure 4 shows the luminescence decay kinetics for NPs and NTs measured at a wavelength of 540 nm. Kinetic curves are generally non-exponential. Lifetimes of excited states calculated from the exponential part of the decay curves are shown in Table 1.

Table 1. Duration of luminescence of films from NPs and NTs on different wavelengths.

Sample	Excitation wavelength		
	510 nm	540 nm	600 nm
NPs (773 K)	τ=6.2 ms	τ=3.0 ms	τ= 6.7 ms
NTs (773 K)	τ=2.5 ms	τ=0.8 ms	τ=6.3 ms

The presented data shows that the lifetimes of the excited states of the defect centers are different as for NPs and for NTs. The obtained spectral results are correlated well with the published data [23], where the luminescence of the anatase structure of NT titanium dioxide is associated with three possible defect states: self-trapped excitons STE, Ti^{3+}/F и F^+. For rutile phase photoluminescence is associated with oxygen vacancies [14]. Oxygen vacancies are important defects in nanocrystalline TiO_2, because the efficiency of electron transport and recombination processes depends on their number. Figure 4 shows the spectra and kinetics of luminescence decay films from NPs and NTs, annealed at T = 1273 K.

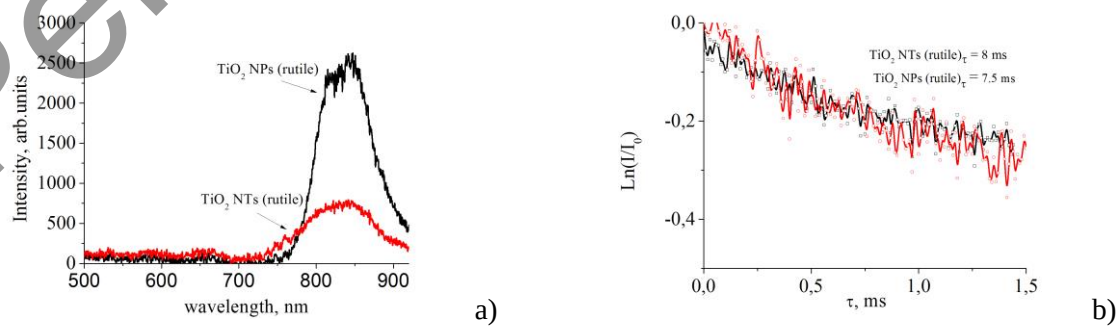

Figure 4. Spectral and kinetic properties of the film annealed at 1273 K.

For both samples luminescence of rutile modification with a maximum range of 850 nm is observed (Fig. 1, a). It should be noted that the light intensity for NPs is much higher than for NTs. Figure 4 (b) also shows the kinetics of luminescence decay of NPs and NTs. Excitation wavelength was 850 nm. Lifetimes of excited states make up 7.5 and 8.0 ms for NPs and NTs respectively. For the investigation of the possibility of using nano-structured films of titanium dioxide in DSSC sandwich structures on the standard method were designed [23] and measured their IV- characteristics which are presented in Figure 6.

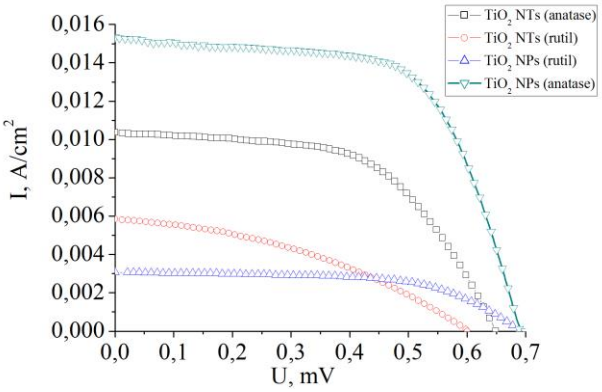

Figure 6. I-V characteristics of DSSC based on TiO_2 films and the dye N719.

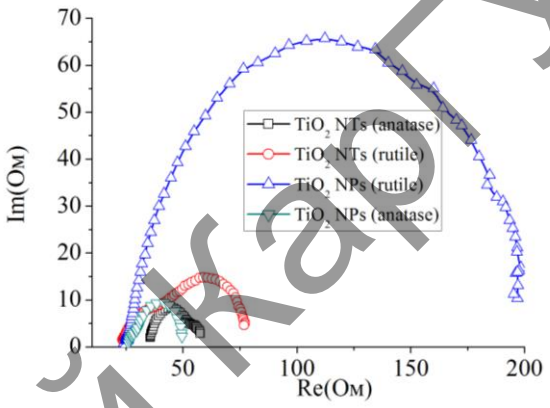

Figure 7. Impedance spectra of DSSC.

Based on the obtained curves of IV- characteristics main photovoltaic solar cell parameters were determined which are presented in Table 3.

Table 3. Photovoltaic properties of DSSC.

Sample	$U_{oc,}$ B	J_{sc}, (A/cm^2)	FF	Efficiency, %
NPs (773 K)	0.69	0.014	0.62	4.10
NPs (1273 K)	0.68	0.003	0.60	1.32
NTs (773 K)	0.65	0.010	0.56	3.80
NTs (1273 K)	0.60	0.005	0.38	1.36

From this tabulated data it is evident that the photovoltaic characteristics of cells based on films from NPs and NTs anatase are higher than for the films of rutile structure. The difference of U_{oc} values for cells based on rutile and anatase is associated with the location of Fermi quasilevel. Figure 7 shows hodographs of impedance in Nyquist coordinates for solar cells based on TiO_2 films. Using the method described in [25, 26] from the impedance spectra were calculated effective diffusion coefficient of *Deff* electrons, the effective speed of k_{eff} recombination, effective lifetime of τ_{eff} electron, resistance of electron transport in the film of R_w titanium dioxide, R_k charge transfer resistance, associated with recombination of electron. The results are shown in Table 4.

Table 4. The electron transport properties of TiO_2 films in the DSSC.

Annealing temperature	D_{eff}	k_{eff} (c^{-1})	τ_{eff} (*c*)	R_k (*Ом*)	R_w (*Ом*)
NPs (anatase)	$9.9*10^{-5}$	14.0	0.07	22.0	*26*
NPs (rutile)	$4.7*10^{-5}$	57.0	0.02	175.0	*26*
NTs(anatase)	$5.5*10^{-5}$	3.6	0.27	17,5	36
NTs ((rutile)	$2.9*10^{-5}$	25.3	0.04	38.0	40

From the tabulated data it is evident that the electron transport resistance in TiO_2 (Rw) of NTs films is higher than in NPs. From the table 4 it is evident that the rate of recombination (*keff*) in the

films based on NTs is less than *keff* cells based on NPs similar modification of TiO_2. This is probably due to SCS manufacturing technology based on NTs. In accordance with the formula $k_{eff}=2N_s k_r$ (*Ns* - density of electrons on the defect levels of the energy (c*m-3*), k_r - recombination rate constant ($cm^3 s^{-1}$) to electrolyte of electrons from TiO_2 defect levels [26]) it can be concluded that in the rutile films of NPs and NTs the concentration of the defects through which recombination processes occur is higher than in anatase.

4. Conclusion

In the paper the spectral and kinetic properties of the photoluminescence films formed from NPs and NTs of titanium dioxide were investigated. For samples annealed at T=773 K, when excited by a nitrogen laser luminescence is observed with a spectrum characteristic of the anatase structure. Annealing of the samples at T=1273 K leads to a long-wavelength shift of the photoluminescence band with maximum at 850 nm wavelength which corresponds to the rutile structure. The researches of the photovoltaic properties sensitized by the dye of solar cells have shown that the anatase-based films have a higher cell efficiencies than the cells with rutile films. It is found that in the films based on NTs the recombination rate is less but the resistance to the electron transport is higher than in the films from NPs. In the rutile films of NPs and NTs the concentration of defects through which the recombination processes occur is higher than in anatase.

5. References

[1] Fujishima A, Honda K 1972 *Nature* **238** 37
[2] Hasan M et al. 2008 *Chemical and Biological Engineering* **1** 92
[3] Ito S, Murakami T N, Comte P 2008 *Thin Solid Films* **516** 4613
[4] Lee J, Sang K, Shin K 2012 *Journal of Industrial and Engineering Chemistry* **18** 19
[5] Yang C 2008 *Applied Surface Science* **23** 2685
[6] Yang J, Mei S, Ferreira J 2001 *Materials Science and Engineering: C* **15** 183
[7] Wu X, Jiang Q Z, Ma Z F 2005 *Solid State Communications* **136** 513
[8] Fujihara K, Kumar A, Jose R 2007 *Nanotechnology* **18** 37
[9] Arcadipane E, Sanz R, Miritello M 2016 *Materials Science in Semiconductor Processing* **42** 24
[10] Mukul D, Hongshan H 2012 *Scanning Electron Microscopy* **27** 537
[11] Mo S D, Ching W Y 1995 *Physical review* **51** 15
[12] Carpa O, Huisman C L, Reller A 2012 *Progress in Solid State Chemistry* **32** 33
[13] Landmann M, Rauls E, Schmidt W G 2012 *Journal of Physics: Condensed Matter* **24** 195503
[14] Ivlev V, Gusev S, Latyshev A 2012 *Condensed Matters and the interphase boundaries* **14** 141
[15] Wang X, Feng Z, Shi J 2010 *Physical Chemistry Chemical Physics* **12** 7083
[16] Nakajimaa H, Mori T 2004 *Journal of applied physics* **96** 1
[17] Serpone N, Lawless D, Khairutdinov R 1995 *Journal Physics Chemystry* **99** 16646
[18] Mercado C, Seeley Z, Bandyopadhyay A 2011 *ACS Applied Materials & Interfaces* **3** 2281
[19] Sanjinés R R, Tang H, Berger H 1994 *Applied Physics* **75** 2945
[20] Lin J, Chen J, Chen X 2010 *Electrochemistry Communications* **12** 1062
[21] Bach U, Lupo D, Comte P, Moser J E and M Gratzel 1998 *Nature* **395** 583
[22] Lin J, Chen J Chen X 2011 *Nanoscale Research Letters* **6** 475
[23] Zhang H, Zhou M, Fu Q 2014 *Nanotechnology* **25** 275603
[24] Brunauer S, Deming L S, Deming W S 1940 *Jour. of the American Chemical Society* **62** 1723
[25] F-Santiago F, Bisquert J, G-Belmonte G 2005 *Solar Energy Materials & Solar Cells*. **87** 117
[26] Adachi M, Sakamoto M, Jiu J 2006 *Journal Physics Chemistry* B **110** 13872